Latent Specificity of Molecular Recognition in Sodium Channels Engineered To Discriminate between Two "Indistinguishable" μ-Conotoxins†

Ronald A. Li,‡ Irene L. Ennis,‡ Gordon F. Tomaselli,‡ Robert J. French,§ and Eduardo Marbán*,‡

Institute of Molecular Cardiobiology, The Johns Hopkins University School of Medicine, Baltimore, Maryland 21205, and Department of Physiology and Biophysics, University of Calgary, Calgary, Alberta, Canada

Received January 11, 2001; Revised Manuscript Received March 9, 2001

ABSTRACT: μ-Conotoxins (μ-CTX) are potent oligopeptide blockers of sodium channels. The best characterized forms of μ-CTX, GIIIA and GIIIB, have similar primary and three-dimensional structures and comparable potencies (IC_{50} ~30 nM) for block of wild-type skeletal muscle Na^+ channels. The two toxins are thus considered to be indistinguishable by their target channels. We have found mutations in the domain II pore region (D762K and E765K) that decrease GIIIB blocking affinity ~200-fold, but reduce GIIIA affinity by only ~4-fold, compared with wild-type channels. Synthetic μ-CTX GIIIA mutants reveal that the critical residue for differential recognition is at position 14, the site of the only charge difference between the two toxin isoforms. Therefore, engineered Na^+ channels, but not wild-type channels, can discriminate between two highly homologous conotoxins. Latent specificity of toxin−channel interactions, such as that revealed here, is a principle worthy of exploitation in the design and construction of improved biosensors.

Voltage-gated Na^+ channels underlie electrical conduction in muscle and nerve. Given their physiological importance, it is not surprising that Na^+ channels are favored targets of various biological toxins. μ-Conotoxins (μ-CTX)[1] are receptor site I sodium channel blockers (*1*) produced by the sea snail *Conus geographus* (*2*−*5*) that specifically inhibit Na^+ flux by physical occlusion of the channel pore (*2*, *6*−*9*). The best studied forms of μ-CTXs, GIIIA and GIIIB, are 22 amino acid peptides with three internal disulfide bonds imparting structural rigidity to the molecules (*10*). The three-dimensional structures of both μ-CTX forms are well-defined (*11*−*14*), making them invaluable tools to probe the uncertain Na^+ channel pore architecture. The amino acid sequences of GIIIA and GIIIB are highly homologous (Figure 1) with only four differences, the most radical of which is a Q-to-R difference at position 14. This imparts to GIIIB an extra net positive charge (+7) compared with GIIIA (+6) at physiological pH. Many of the positive charges have been shown to be important for potent toxin block of the Na^+ channel (*14*−*17*).

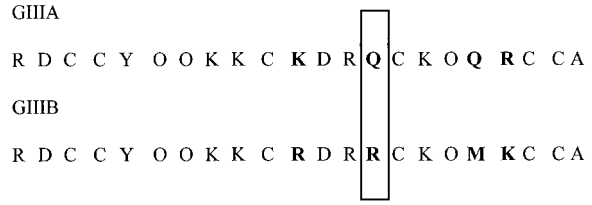

FIGURE 1: Amino acid sequences of μ-conotoxin GIIIA and GIIIB. Both forms of the toxin contain 22 amino acids. At neutral pH, GIIIA and GIIIB carry a net charge of +6 and +7, respectively. The two peptide−toxins differ at four positions, and the corresponding residues are in bold. The nonconservative Q-to-R difference (enclosed in the box) located at position 14 gives GIIIB an extra net positive charge. Note that O is used here to represent 4-*trans*-hydroxyproline.

On the basis of the similarities in structure and blocking potency, GIIIA and GIIIB have been generally considered to be indistinguishable at the electrophysiological level. Indeed, no native or mutated Na^+ channels have been shown to be capable of discriminating between the two toxin isoforms. We have recently identified two negatively charged residues (D762 and E765) located in the domain II (DII) P-S6 linker of the rat skeletal muscle (μ1) Na^+ channel that are critical for μ-CTX GIIIB block (*18*, *19*). Here, we report that mutant Na^+ channels with either of these channel residues converted to lysine (i.e., D762K and E765K) discriminate strongly between the two toxin isoforms. Mutant cycle analysis, applied to further experiments with mutant μ-CTX derivatives, allowed us to identify the variant residues at position 14 of the toxins (i.e., GIIIA-Q14, GIIIB-R14) as the basis for the discrimination.

EXPERIMENTAL PROCEDURES

Site-Directed Mutagenesis and Heterologous Expression. μ1 sodium channel (*20*) mutants were created using poly-

† This work was supported by the National Institutes of Health (R01 HL-52768 to E.M. and R01 HL-50411 to G.F.T.) and by operating funds from the Medical Research Council/Canadian Institutes of Health Research (to R.J.F.). R.A.L. is the recipient of a fellowship award from the Heart and Stroke Foundation of Canada. I.L.E. is supported by a fellowship award from FOMEC, Argentina. R.J.F. receives salary support as an MRC/CIHR Distinguished Scientist and an Alberta Heritage Foundation for Medical Research Medical Scientist. E.M. holds the Michel Mirowski, M.D. Professorship of Cardiology of the Johns Hopkins University.

* Address correspondence to this author at the Institute of Molecular Cardiobiology, The Johns Hopkins University School of Medicine, 720 Rutland Ave., Ross 844, Baltimore, MD 21205. E-mail: marban@jhmi.edu.

‡ The Johns Hopkins University School of Medicine.

§ University of Calgary.

[1] Abbreviations: μ1, rat skeletal muscle sodium channel; μ-CTX, μ-conotoxin; WT, wild type; $\Delta\Delta G$, coupling energy.

10.1021/bi010077f CCC: $20.00
Published on Web 04/25/2001

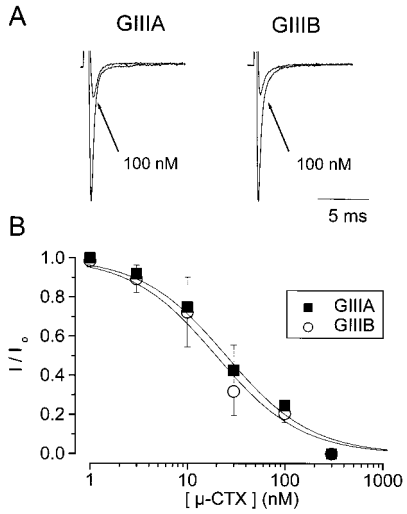

FIGURE 2: Comparison of block of rat skeletal muscle (μ1) Na^+ channels by μ-CTX GIIIA and GIIIB. (A) Representative raw current records of μ1 channels elicited by depolarization to −10 mV from a holding potential of −100 mV in the absence and presence of 100 nM μ-CTX GIIIA (left panel) and GIIIB (right panel). Peak currents were normalized to those recorded under toxin-free conditions for comparison. (B) The dose−response relationship for GIIIA (solid squares) and GIIIB (open circles) block of μ1 and E765C (open triangles) channels. Normalized peak Na^+ currents at −10 mV were plotted as a function of extracellular toxin concentrations. Data points were fitted with a single-site binding isotherm to estimate the IC_{50} of μ1 channels for block by GIIIA or GIIIB (see Experimental Procedures). Data are plotted as mean ± SEM. IC_{50} values estimated were 30.7 ± 6.2 nM, $n = 6$, and 29.7 ± 8.6 nM, $n = 7$, for GIIIA and GIIIB, respectively. The two values were not statistically different ($p > 0.05$).

merase chain reaction (PCR) and expressed in tsA-201 cells as previously described (*21*). The desired mutants were confirmed by DNA sequencing. Lipofectamine Plus kit (Gibco-BRL, Gaithersburg, MD) was used for transfection. DNA encoding the WT or mutant α-subunit (1 μg/60 mm dish) was added to the cells with lipofectamine. Transfected cells were incubated at 37 °C in a humidified atmosphere of 95% O_2−5% CO_2 for 48−72 h before electrical recordings.

Synthesis of Point-Mutated Derivatives of μ-CTX GIIIA. Toxin derivatives were synthesized as previously described (*15*, *22*). Briefly, solid-phase synthesis was performed on a polystyrene-based Rink amide resin using 9-fluorenylmethoxycarbonyl chemistry. Synthesized peptides were air-oxidized and HPLC-purified. The resulting peptides eluted as a single dominant peak. Peptide composition was verified by quantitative amino acid analysis and/or mass spectroscopy. One-dimensional proton NMR spectra of toxin derivatives (including Q14D) synthesized and isolated in this way have revealed no evidence of improper folding.

Electrophysiology and Data Analysis. Electrophysiological recordings were performed using the whole-cell patch clamp technique (*23*). Transfected cells were identified by epifluorescence microscopy. Pipet electrodes had final tip resistances of 1−3 MΩ. Recordings were performed at room temperature in a bath solution containing 140 mM NaCl, 5 mM KCl, 2 mM $CaCl_2$, 1 mM $MgCl_2$, 10 mM HEPES, and 10 mM glucose, pH adjusted to 7.4 with NaOH. Designated amounts of μ-CTX (GIIIA, GIIIB, and point-mutated GIIIA) were added to the bath when required. The internal recording solution contained 35 mM NaCl, 105 mM CsF, 1 mM $MgCl_2$, 10 mM HEPES, and 1 mM EGTA, pH adjusted to 7.2 with CsOH. All chemicals were purchased from Sigma unless otherwise specified.

Toxin was superfused continuously during the experiment at flow rates of 10−20 mL/min (bath volume = 150 μL). Washout began only after the peak currents had reached a steady-state level. Currents were analyzed using custom-written software. Half-blocking concentrations (IC_{50}) for μ-CTX were determined by least-squares fits of the dose−response data to a binding isotherm of the form

$$I/I_O = 1/\{1 + ([\text{toxin}]/IC_{50})\}$$

where IC_{50} is the half-blocking concentration and I_O and I are the peak currents measured from a step depolarization to −10 mV from a holding potential of −100 mV before and during application of the blocker, respectively.

For mutant cycle analysis, coupling/interaction energies ($\Delta\Delta G$) for various mutant toxin−channel pairs were calculated from the equilibrium IC_{50} values using the equation:

$$\Delta\Delta G = \Delta G_1 - \Delta G_2$$

$$\Delta G_1 = G^{\text{mutated toxin−WT channel}} - G^{\text{WT toxin−WT channel}} = RT(\ln IC_{50}^{\text{mutated toxin−WT channel}} - \ln IC_{50}^{\text{WT toxin−WT channel}})$$

$$\Delta G_2 = G^{\text{mutated toxin−mutated channel}} - G^{\text{WT toxin−mutated channel}} = RT(\ln IC_{50}^{\text{mutated toxin−mutated channel}} - \ln IC_{50}^{\text{WT toxin−mutated channel}})$$

R is the gas constant and T is the temperature. The standard errors for $\Delta\Delta G$ were estimated by dividing the square root of the sum of the variances of the RT ln IC_{50} means by the square root of the degree of freedom.

Kinetic analysis of toxin block was performed as previously described (*18*).

All data are reported as mean ± SE. Statistical significance was determined using a paired Student's t-test at the 5% level.

RESULTS

μ-CTX GIIIA and GIIIB Block WT μ1 Na^+ Channels with Similar Affinity. We initially compared the susceptibilities of wild-type (WT) μ1 Na^+ channels to block by μ-CTX GIIIA and GIIIB. Figure 2A shows typical Na^+ currents of WT channels recorded in the absence and presence of GIIIA (left panel) and GIIIB (right panel). Application of 100 nM GIIIA blocked peak current (I_{Na}) of WT channels to 24.7 ± 4.9% ($n = 4$) of that recorded under toxin-free conditions. Addition of 100 nM GIIIB displayed identical block ($p > 0.05$), with I_{Na} reduced to 20.5 ± 4.4% ($n = 5$) of the control level. Figure 2B shows the dose−response curves of WT channels for block by GIIIA (solid squares) or GIIIB (open circles). Consistent with the premise that μ-CTXs block Na^+ channels with 1:1 stoichiometry (*2*, *6*−*9*, *24*), both data sets were well fitted with a binding isotherm assuming a Hill coefficient of 1. The half-blocking concentrations (IC_{50}) estimated from these binding curves, 30.7 ± 6.2 nM, $n = 6$,

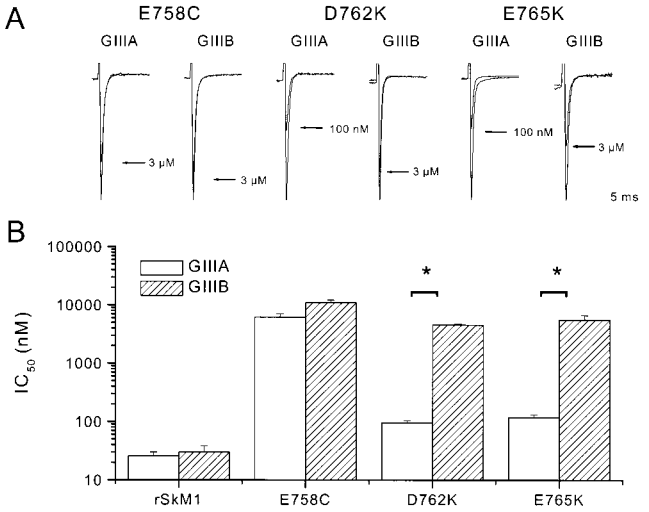

FIGURE 3: Effects of point mutations on channel sensitivities to μ-CTX GIIIA and GIIIB. (A) Representative Na^+ currents through E758Q, D762K, and E765K channels elicited by depolarization to −10 mV from a holding potential of −100 mV in the absence and presence of μ-CTX GIIIA and GIIIB as indicated by arrows. Current amplitudes were normalized to the peak current for each mutant in the absence of μ-CTX. (B) Bar graphs summarizing the IC_{50} values of WT, E758Q, D762K, and E765K channels for block by μ-CTX GIIIA and GIIIB. Though insensitive to GIIIB, D762K and E765K channels were relatively sensitive to GIIIA. In contrast, E758C channels were insensitive to both μ-CTX isoforms. Asterisks indicate statistically significant differences ($p < 0.05$).

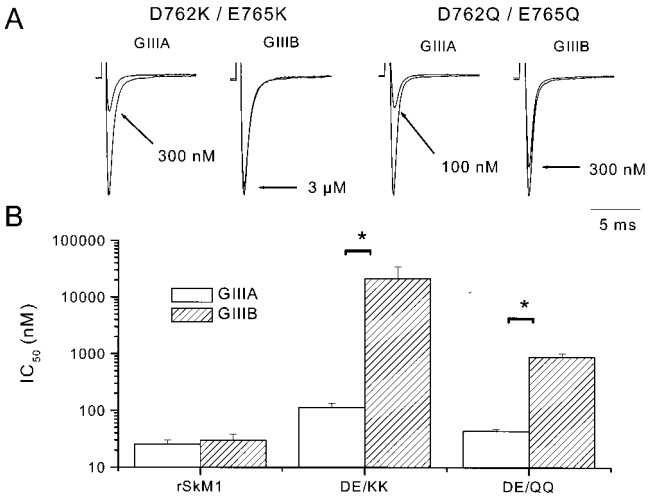

FIGURE 4: Effects of double mutations on channel block by μ-CTX GIIIA and GIIIB. (A) Representative Na^+ currents through D762K/E765K and D762Q/E765Q double mutant channels elicited by depolarization to −10 mV from a holding potential of −100 mV in the absence and presence of μ-CTX as indicated by arrows. Current amplitudes were normalized to the peak current recorded under control conditions. (B) Bar graphs summarizing IC_{50}s for GIIIA and GIIIB block of the same channels shown in (A). Like their single mutant counterparts, both D762K/E765K and D762Q/E765Q were insensitive to GIIIB yet sensitive to GIIIA. Note that the effect of combining the mutations D762K and E765K on GIIIB block was additive relative to the singles. The data presented are the mean ± SEM from three to six individual determinations. Asterisks indicate statistically significant differences ($p < 0.05$).

and 29.7 ± 8.6 nM, $n = 7$, for GIIIA and GIIIB, respectively, were statistically identical.

Differential Sensitivities to GIIIA and GIIIB Block of D762K and E765K Channels. We previously reported that the negatively charged domain II residues E758, D762, and E765 are critical for the binding of μ-CTX GIIIB to Na^+ channels (8, *18*, *19*). Here we compared GIIIA and GIIIB block of Na^+ channels mutated at these positions. Figure 3A shows representative current records of E758C, D762K, and E765K channels measured with or without toxins. Cysteine substitution of E758 dramatically reduced block by both GIIIA ($IC_{50} = 6.2 \pm 0.8$ μM, $n = 4$) and GIIIB ($IC_{50} = 10.9 \pm 1.2$ μM, $n = 3$), consistent with previous studies of charge neutralization of this pore residue with either GIIIA (*7*) or GIIIB (*8*). Notably, the D762K and E765K mutants were ~200-fold less sensitive to GIIIB (D762K = 4.5 ± 0.2 μM, $n = 3$; E765K = 5.6 ± 1.0 μM, $n = 5$) than WT channels. However, these mutants displayed only a modest increase (~4-fold) in IC_{50} for block by GIIIA (D762K = 95.9 ± 9.0 nM, $n = 5$; E765K = 117.3 ± 14.4 nM, $n = 7$). These significant differences in sensitivities to GIIIA and GIIIB indicate that the DII P-S6 mutations have conferred upon Na^+ channels the ability to discriminate between the two toxin forms despite the nearly indistinguishable toxin backbones (*11*−*13*). Consistent with these results, the double mutant D762K/E765K was insensitive to GIIIB block ($IC_{50} = 21.4 \pm 13.0$ μM, $n = 3$) but quite sensitive to GIIIA ($IC_{50} = 113.3 \pm 20.6$ nM, $n = 3$) (Figure 4). Similarly, D762Q/E765Q was insensitive to GIIIB ($IC_{50} = 878.8 \pm 145.1$ nM, $n = 7$) but relatively sensitive to GIIIA ($IC_{50} = 43.6 \pm 3.3$ n M, $n = 3$) (Figure 4).

Differences in GIIIA and GIIIB Block Reside in Toxin Position 14. As mentioned, GIIIA and GIIIB differ only at four positions (cf. Figure 1), with a single charge change (i.e., Q to R) at position 14, giving GIIIB an extra net positive charge relative to GIIIA. On the basis of this molecular difference, we postulated that the different binding affinities of GIIIA and GIIIB to D762K and E765K channels originate from this amino acid difference at position 14. To test this hypothesis, we chemically synthesized the GIIIA-based toxin derivatives Q14R and Q14D and determined their IC_{50}s for block of WT and the DII P-S6 lysine-substituted channels. Figure 5 summarizes these results. The substitution Q14R did not significantly affect GIIIA binding to WT channels ($IC_{50} = 47.4 \pm 8.1$ nM, $n = 4$; $p > 0.05$). In contrast, binding of GIIIA-Q14R to D762K and E765K channels was dramatically reduced ($p < 0.05$). The IC_{50}s estimated were 1.4 ± 0.1 μM, $n = 3$, and 1.7 ± 0.7 μM, $n = 3$, for D762K and E765K, respectively. These observations were consistent with the notion that GIIIA-Q14R mimics GIIIB, and the Q-to-R difference underlies the differential sensitivities of D762K and E765K channels to GIIIA and GIIIB toxins. In addition, these results also suggest the presence of a prominent electrostatic (repulsive) component of interactions between R14 and the channel residues K762 and K765. In support of this idea, replacement of Q14 with the negatively charged aspartate (i.e., GIIIA-Q14D) decreased toxin binding to WT channels by approximately 70-fold ($IC_{50} = 2.2 \pm 0.4$ μM, $n = 3$, $p < 0.05$), as if the substituted aspartate was electrostatically repelled by anionic channel residues. More interestingly, blocking efficacy of GIIIA-Q14D was significantly ($p < 0.05$) improved when applied to D762K ($IC_{50} = 0.6 \pm 0.1$ μM, $n = 4$) and E765K ($IC_{50} = 1.1 \pm 0.1$ μM, $n = 3$) channels (Figure 5), probably as a result of attractive electrostatic forces between D14 and the positively charged, substituted lysines in the DII P-S6 linker of the channel.

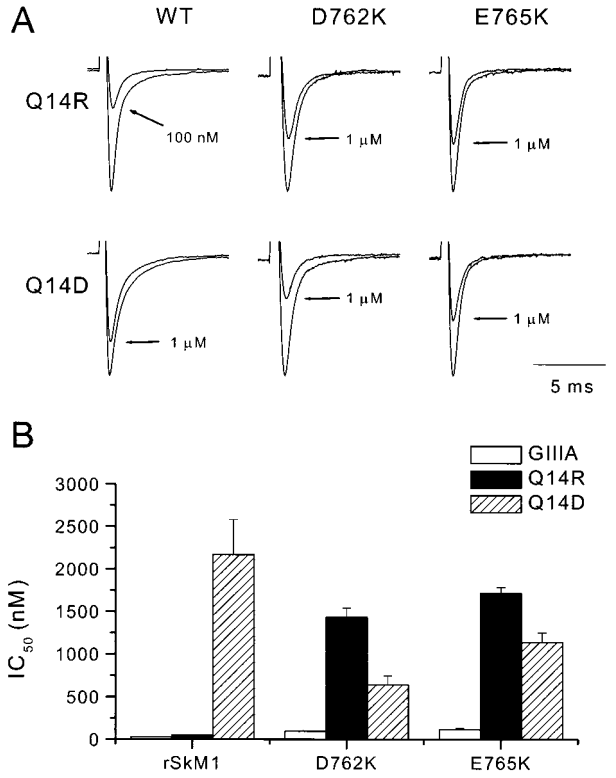

FIGURE 5: Block of WT, D762K, and E765K channels by μ-CTX GIIIA, GIIIA-Q14R, and GIIIA-Q14D. (A) Representative Na^+ current tracings of WT, D762K, and E765K channels (test pulse = −10 mV, holding potential = −100 mV) recorded with or without toxin as indicated by arrows. Control peak currents were normalized. (B) Bar graphs summarizing the half-blocking concentrations (IC_{50}) for block by GIIIA, GIIIA-Q14R, and GIIIA-Q14D of the same channels shown in (A). The data presented are the mean ± SEM from three to six individual determinations.

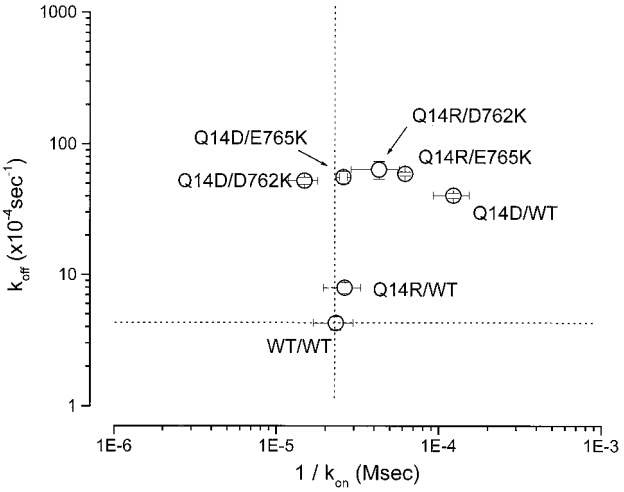

FIGURE 6: Effects of Q14R and Q14D on the blocking kinetics of μ-CTX GIIIA. Logarithmic plot of the dissociation rate constants (k_{off}) versus the reciprocal of the association rate constants (k_{on}). The horizontal and vertical dotted lines represent the levels of $1/k_{on}$ and k_{off} for the WT channels, respectively. The kinetic equilibrium constants (K_D) derived from these data display the same trend as the corresponding IC_{50} values. These data are summarized and compared in Table 1.

Figure 6 further demonstrates the effects of Q14R and Q14D on the kinetics of GIIIA block. The time course of onset (or offset) of toxin block was fitted with a single-exponential function, and the resulting time constants were used to derive the corresponding toxin association and dissociation rate constants (i.e., k_{on} and k_{off}) and kinetic equilibrium constants (K_D) (*18*). As anticipated, the blocking kinetics of WT channels by GIIIA-Q14R were similar to those of WT GIIIA. However, application of this derivative to D762K and E765K channels significantly increased k_{off} by ~15-fold, with k_{on} only modestly affected (~2-fold difference). When applied to WT channels, GIIIA-Q14D affected both k_{on} and k_{off} (5-fold decrease and 10-fold increase, respectively). Application of GIIIA-Q14D to the lysine-substituted channels restored wild-type k_{on}, possibly due to the creation of new attractive forces. These combinations (i.e., K762/D14 and K765/D14), however, had no effects on k_{off}. All kinetically derived K_Ds are summarized in Table 1. They were generally comparable to the steady-state IC_{50}s and displayed the same trend of changes despite different potential sources of error in these two complementary methods of analysis.

Interaction Energies of Q14R and Q14D with K762 and K765. To quantify the interactions between the DII P-S6 channel residues K762 and K765 and μ-CTX at position 14, coupling energies ($\Delta\Delta G$) between these sites were calculated from the experimentally derived IC_{50}s using thermodynamic mutant cycle analysis (see Experimental Procedures and ref *25* for review) (Figure 7). The $\Delta\Delta G$s calculated for interactions between GIIIB and the mutant channels D762K and E765K relative to GIIIA were −2.3 ± 0.2 and −2.3 ± 0.2 kcal/mol, respectively. Such negative changes represent a loss of coupling energies when GIIIB instead of GIIIA was applied to these channels, but it is not possible, a priori, to assign the coupling to any particular pair of residues. For the interacting pairs D762K/GIIIA-Q14R and E765K/GIIIA-Q14R, $\Delta\Delta G$s were −1.3 ± 0.1 and −1.2 ± 0.1 kcal/mol, respectively, also representing a loss of coupling energies by the introduced pairs relative to the native ones. These data indicate that the D762K/GIIIA-Q14R and E765K/GIIIA-Q14R pairs each account for ~60% of the energy lost when GIIIB was tested against the respective channel mutant. In contrast, the interacting pairs D762K/GIIIA-Q14D and E765K/GIIIA-Q14D displayed $\Delta\Delta G$ of +1.5 ± 0.1 and +1.3 ± 0.1 kcal/mol, respectively, reflecting gains of coupling energies by the oppositely charged pairs. Taken together, these results suggest that both D762 and E765 have a strong interaction with the toxin residue at position 14, which includes an important electrostatic component.

DISCUSSION

Channel Mutants D762K and E765K Discriminate between Conotoxins GIIIA and GIIIB. We compared block of WT and mutant Na^+ channels by μ-CTX GIIIA and GIIIB, two forms of the snail toxin that previously were thought to be functionally equivalent. In contrast to WT Na^+ channels, the mutations D762K and E765K discriminate between GIIIA and GIIIB. Since the two toxin isoforms are so similar, yet mutations of the DII P-S6 residues but not the nearby E758 (four residues amino-terminal to D762) abolished GIIIB block while retaining sensitivity to GIIIA, high-affinity toxin−channel interactions must be highly localized. The same line of reasoning argues against major nonspecific conformational disruption of the channel as the basis of the changes in toxin affinity. Furthermore, the observation that combining the mutations D762K and E765K further weak-

Table 1: Comparison of Kinetically Derived K_D and Equilibrium IC_{50} of WT GIIIA and Its Derivatives Q14R and Q14D

channel/toxin	$K_D = k_{off}/k_{on}$ (nM)	$K_{D,channel/toxin}/K_{D,WT/WT}$	IC_{50} (nM)	$IC_{50,channel/toxin}/IC_{50,WT/WT}$
WT/WT	$(1.0 \pm 0.4) \times 10^2$	1.0	$(3.0 \pm 0.6) \times 10$	1.0
WT/Q14R	$(1.9 \pm 0.2) \times 10^2$	1.9	$(4.7 \pm 0.8) \times 10$	1.5
WT/Q14D	$(4.9 \pm 1.3) \times 10^3$	46.9	$(2.2 \pm 0.4) \times 10^3$	71.9
D762K/Q14R	$(2.5 \pm 0.7) \times 10^3$	24.4	$(1.4 \pm 0.1) \times 10^3$	47.7
D762K/Q14D	$(7.4 \pm 1.2) \times 10^2$	7.1	$(6.4 \pm 1.1) \times 10^2$	20.9
E765K/Q14R	$(3.5 \pm 1.1) \times 10^3$	32.8	$(1.7 \pm 0.7) \times 10^3$	56.0
E765K/Q14R	$(1.4 \pm 0.1) \times 10^3$	13.7	$(1.1 \pm 0.1) \times 10^3$	37.2

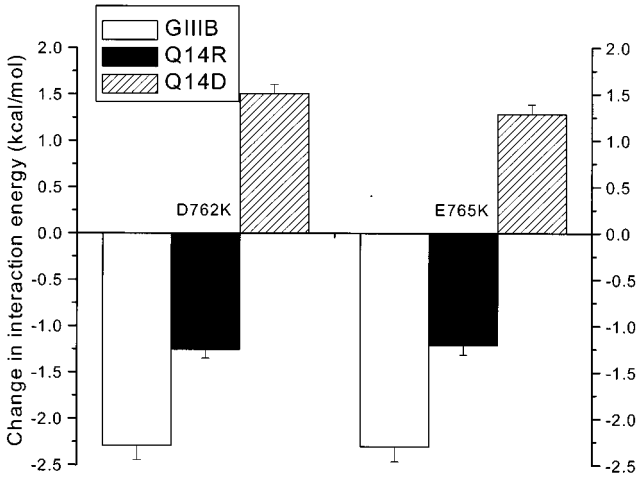

FIGURE 7: Interaction energies estimated from mutant cycle analysis between DII P-S6 residues and various μ-CTXs. Loss of coupling energy by either the D762K/Q14R or E765K/Q14R pairs accounts for approximately 60% of the energy loss of GIIIB binding to these channels relative to GIIIA.

ened GIIIB block, relative to either of the single mutations, suggests that both negative charges must be present simultaneously for optimal GIIIB−channel interactions and that each may have its optimal partners in the toxin. However, the double mutant (i.e., D762K/E765K) displayed only a ~4-fold further reduction in toxin binding affinity compared to the singles, which were each ~200-fold less sensitive to GIIIB than were the WT channels. Thus, it seems possible that the DII P-S6 residues share common interacting toxin sites and to some extent provide alternate interactions with the toxin. Indeed, this idea is consistent with our finding that both D762 and E765 associate closely with Q(R)14.

Molecular Interactions between Q14 and DII P-S6 Residues. At first glance, our previous finding that D762 and E765 are critical for GIIIB binding (*18*) appeared inconsistent with the earlier data of Chahine et al. (*26*). These authors reported that the charge-neutralized double mutant D762Q/E765Q displayed a wild-type GIIIA-blocking phenotype and concluded that these DII residues did not participate in binding. Our present data rationalize this apparent discrepancy as a consequence of the different toxins used in the two studies [GIIIA by Chahine et al. (*26*) vs our GIIIB]. Using toxin derivatives in combination with mutant cycle analysis, we demonstrate here that the toxin residue at position 14 can interact strongly with both D762 and E765. A somewhat weaker interaction of toxin residue 14 with DII (residue 759) has been reported recently (*27*). Our present observations provide an explanation as to why D762K and E765K channels were insensitive to GIIIB but not GIIIA, as electrostatic repulsion might exist between the lysine-substituted DII P-S6 residues and GIIIB-R14, thereby preventing it from binding optimally to the channel receptor. This repulsion, however, would not exist with the neutral Q14 in GIIIA.

Several observations suggest that steric factors, as well as electrostatic interactions, may contribute to the differences in blocking kinetics seen for the various toxin−channel pairs. Previously, we reported that restoration of native charge in channel mutants D762C and E765C using sulfhydryl-modifying reagents did not restore high-affinity GIIIB block (*18*). In our present data, GIIIA-Q14R shows a modest decrease in IC_{50} (~1.5-fold) compared to WT GIIIA (Table 1). Further, association rates vary approximately 10-fold among five toxin-channel pairs in which μ-CTX residue 14 has the same charge as one, or both, of the DII P-S6 residues 762 or 765 (see Figure 6; Q14D/WT, Q14D/D762K, Q14D/E765K, Q14R/D762K, and Q14R/E765K). In contrast, dissociation rates, which are approximately 10-fold faster than for the WT/WT pair, show little variation within this group. Testing with μ-CTX GIIIB, a range of more than 10-fold in dissociation rates was observed with substitutions for D762 or E765, but only D762K showed a substantial change in association rate [see Figure 7 in Li et al. (*18*)]. The common feature of the two data sets is that any mutation, which generates a charge match between toxin residue 14 and one of channel residues 762 or 765, is associated with a decrease in affinity. Observed changes in affinity can invariably be attributed, in part, to increases in dissociation rate, with variable changes—usually decreases—in the association rate. Although electrostatic interactions seem to be crucial, a complete understanding of the toxin−channel interaction will require an analysis of the influence of side chain size, flexibility, and conformation.

Overall, interactions of the toxin residue at position 14 with either D762 or E765 account for approximately 60% of the binding energy lost when GIIIB was tested against the mutant channels. It is therefore reasonable to propose that the difference in sensitivities between the two toxin isoforms largely resides in the Q-to-R difference at position 14. The rest of the energy loss may be attributed to other electrostatic and nonelectrostatic interactions existing between Q14R and/or the other three amino acid differences between GIIIA and GIIIB (i.e., K11R, Q18M, R19K) and other channel residues. At this point, it is not clear why the extra charge provided by R14 should not confer on GIIIB a higher affinity than that of GIIIA. A more detailed knowledge of the structure of the toxin channel complex may be required to resolve this issue.

Structural Implications of the Channel Pore. Three-dimensional structures of GIIIA and GIIIB studied by 2D ^{1}H nuclear magnetic resonance (NMR) spectroscopy reveal that the two toxin forms have essentially identical three-dimensional backbone structures (*12*, *13*). In GIIIB, R13,

R14 (Q14 in GIIIA), K16, Hyp17, and K19 (R19 in GIIIA) are clustered on one surface (approximately 17 × 23 Å) of the toxin molecule formed by a distorted helical segment which spans residues 13−22 (*13*), while R8, K9, K11, and D12 form a linker between a β-hairpin and the helix (*14*). It is likely that this helical face of the toxin docks the channel receptor (*13*, *14*). Indeed, R13, K16, Hyp17, and R19 all make important contributions to the potent blocking efficacy of the toxin (*11*, *14*−*16*, *22*, *27*, *28*). Taken together with the strong couplings between Q(R)14 and the DII P-S6 channel residues D762 and E765 demonstrated in the present work, these observations strongly suggest a close association between the toxin helical face and the DII pore-lining residues. In further support of this toxin−channel docking model, we have recently shown that DII P-S6 residues interact with the toxin sites K16 and R19, albeit with different interaction energies, while DIII-D1241 interacts only with K16 (*28*, *29*). These data, interpreted in light of the known toxin structure, further support a clockwise arrangement of the four Na^+ channel domains as viewed from the extracellular side (*28*).

At first glance, it seems possible that the DII channel residues that interact strongly with μ-CTX (i.e., E758, D762, and E765) also form an α-helix, as they are exposed to the aqueous pore and are separated from the next residue by three or four amino acids. However, electrical distances studied by single-channel recordings reveal that D762 and E765 dip back into the membrane, suggesting that these residues are more likely to form a loop (*19*). Further mutagenesis experiments involving other residues in this region are required to distinguish between these possibilities.

It should be noted that implicit in our mutant cycle analysis and data interpretation is the assumption that the mutant toxins bind in an orientation similar to that of the WT toxin. Mutant cycle analysis identifies only interdependent mutational effects on toxin binding. The simplest, but not the only, interpretation is that two sites at which mutations are interdependent interact directly with each other. Different side chain conformations or interactions might affect toxin binding, or the creation of new interactions or cancellation of previously existing ones other than at the sites of the mutations could confound our analysis. Our present data do not allow us to exclude these possibilities, but from a pragmatic viewpoint, the central biological concept would not be affected (i.e., that of engineered specificity of toxin block).

Latent Specificity. The channels reported here (i.e., K762, K765, *K762*/*K765*, and Q762/Q765) that discriminate between the GIIIA and GIIIB forms of μ-CTX are bioengineered channels. However, inspection of the primary sequences of other sodium channel subtypes reveals that some native isoforms have analogous residues at the sequence-aligned positions in DII. For instance, while D762 and E765 are conserved in the rat brain 1, 2, and 3 and human and rat skeletal muscle and heart, as well as the electric eel Na^+ channels, the human neuronal and the sea anemone isoforms have arginine or glutamine analogous to the mutations studied at the equivalent position of 765 in μ1. Although these channel isoforms have not yet been tested electrophysiologically for sensitivity to GIIIA and GIIIB, it seems possible that *Conus* snails have evolved the two toxin forms (and other components of the venom) to target more broadly different channel isoforms in prey. In any case, the concept of "latent specificity" is apparent: proteins can be engineered such that their ability to recognize or distinguish specific ligands can be rendered highly specific even in the absence of inherent specificity.

CONCLUSION

In summary, we conclude that the DII P-S6 mutations, D762K and E765K, confer on μ1 Na^+ channels the unique ability to discriminate between the two extremely similar forms of μ-CTX, namely, GIIIA and GIIIB. We have demonstrated that the underlying basis for such discrimination lies largely in the intimate interactions between Q14 of GIIIA (or R14 of GIIIB) and the channel residues D762 and E765. The promiscuity of the wild-type channels contrasts with the mutant channels' remarkable ability to discriminate between the two μ-conotoxins. This suggests a general principle of latent specificity, in which the backbone structure of a receptor possesses the inherent capacity, as the result of discrete, local substitution(s), to display dramatically different selectivity among similar ligands. Here, a natural, high-affinity toxin receptor has been re-engineered to distinguish between two closely related, naturally occurring toxin molecules. Such manipulation of protein−protein interfaces may lead to improved biosensors for toxins and other small molecules.

ACKNOWLEDGMENT

We thank Drs. Harry Fozzard and Samuel Dudley for helpful discussions regarding mutant cycle analyses and for making available the toxin derivatives Q14R and Q14D.

REFERENCES

1. Catterall, W. A. (1988) Structure and function of voltage-sensitive ion channels, *Science 242*, 50−61.
2. Cruz, L. J., Gray, W. R., Olivera, B. M., Zeikus, R. D., Kerr, L., Yoshikami, D., and Moczydlowski, E. (1985) Conus geographus toxins that discriminate between neuronal and skeletal muscle sodium channels, *J. Biol. Chem. 260*, 9280−9288.
3. Gray, W. R., Olivera, B. M., and Cruz, L. J. (1988) Peptide toxins from venomous Conus snails, *Annu. Rev. Biochem. 57*, 665−700.
4. Nakamura, H., Kobayashi, J., Ohizumi, Y., and Hirata, Y. (1983) Isolation and amino acid compositions of geographutoxin I and II from the marine snail *Conus geographus Linne*, *Experientia (Basel) 39*, 590−591.
5. Olivera, B. M., Rivier, J., Clark, C., Ramilo, C. A., Corpuz, G. P., Abogadie, F. C., Mena, E. E., Woodward, S. R., Hilliyard, D. R., and Cruz, L. J. (1990) Diversity of Conus neuropeptides, *Science 249*, 257−263.
6. Moczydlowski, E., Olivera, B. M., Gray, W. R., and Strichartz, G. R. (1986) Discrimination of muscle and neuronal Na-channel subtypes by binding competition between [^{3}H]saxitoxin and μ-conotoxins, *Proc. Natl. Acad. Sci. U.S.A. 83*, 5321−5325.
7. Dudley, S. C., Jr., Hannes, T., Lipkind, G., and Fozzard H. A. (1995) A μ-Conotoxin-Insensitive Na^+ Channel Mutant: Possible localization of a binding site at the outer vestibule, *Biophys. J. 69*, 1657−1665.
8. Li, R. A., Tsushima, R. G., Kallen, R. G., and Backx, P. H. (1997) Critical pore residues for μ-conotoxin binding to rat skeletal muscle Na^+ channel, *Biophys. J. 73*, 1874−1884.
9. Yanagawa, Y., Abe, T., and Satake, M. (1986) Blockade of [^{3}H]lysine-tetrodotoxin binding to sodium channel proteins by conotoxin GIII, *Neurosci. Lett. 64*, 7−12.

10. Hidaka, Y., Sato, K., Nakamura, H., Ohizumi, Y., Kobayashi, J., and Shimonishi, Y. (1990) Disulfide pairings in geographutoxin I, a peptide neurotoxin from *Conus geographus*, *FEBS Lett. 264*, 29−32.
11. Sato, S., Nakamura, H., Ohizumi, Y., Kobayashi, J., and Hirata, Y. (1983) The amino acid sequences of homologous hydroxyproline-containing myotoxins from the marine snail Conus geographus venom, *FEBS Lett. 155*, 277−280.
12. Lancelin, J. M., Knoda, D., Tate, S., Yanagawa, Y., Abe, T., Satake, M., and Inagaki, F. (1991) Tertiary structure of conotoxin GIIIA in aqueous solution, *Biochemistry 30*, 6908−6916.
13. Hill, J. M., Alewood, P. F., and Craik, D. J. (1996) Three-dimensional solution structure of μ-conotoxin GIIIB, a specific blocker of skeletal muscle sodium channels, *Biochemistry 35*, 8824−8835.
14. Wakamatsu, K., Kohda, D., Hatanaka, H., Lancelin, J. M., Ishida, Y., Oya, M., Nakamura, H., Inagaki, F., and Sato, K. (1992) Structure−activity relationships of μ-conotoxin GII-IA: structure determination of active and inactive sodium channel blocker peptide by NMR and simulated annealing calculations, *Biochemistry 31*(, 12577−12584.
15. Becker, S., Prusak-Sochazewski, E., Zamponi, G., Beck-Sickinger, A. G., Gordon, R. D., and French, R. J. (1992) Action of derivatives of μ-conotoxin GIIIA on sodium channels. Single amino acid substitutions in the toxin separately affect association and dissociation rates, *Biochemistry 31*, 8229−8238.
16. Chahine, M., Chen, L.-Q., Fotouhi, N., Walsky, R., Fry, D., Horn, R., and Kallen, R. G. (1995) Characterizing the μ-Conotoxin binding site on Na channel with toxin analogues and channel mutations, *Recept.Channels 3*, 164−174.
17. Sato, K., Ishida, Y., Wakamatsu, K., Kato, R., Honda, H., Ohizumi, Y., Nakamura, H., Ohya, M., Lancelin, J. M., Kohda, D., and Inagaki, F. (1991) Active site of μ-Conotoxin GIIIA, a peptide blocker of muscle sodium channels, *J. Biol. Chem. 266*, 16989−16991.
18. Li, R. A., Ennis, I., Velez, P., Tomaselli, G. F., and Marbán, E. (2000) Novel structural determinants of μ-conotoxin (GIIIB) block in rat skeletal muscle (μ1) Na^+ channels, *J. Biol. Chem. 275*, 27551−27558.
19. Li, R. A., Velez, P., Chiamvimonvat, N., Tomaselli, G. F., and Marbán, E. (2000) Charged residues between selectivity filter and S6 segments contribute to the permeation phenotype of the sodium channel, *J. Gen. Physiol. 115*, 81−92.
20. Trimmer, J. S., Cooperman, S. S., Tomiko, S. A., Zhou, J., Crean, S. M., Boyle, M. B., Kallen, R. G., Sheng, Z., Barchi, R. L., Sigworth, F. J., Goodman, R. H., Agnew, W. S., and Mandel, G. (1989) Primary structure and functional expression of a mammalian skeletal muscle sodium channel, *Neuron 3*, 33−49.
21. Yamagishi, T., Janecki, M., Marban, E., and Tomaselli, G. F. (1997) Topology of the P segments in the sodium channel pore revealed by cysteine mutagenesis, *Biophys. J. 73*, 195−204.
22. Chang, N. S., French, R. J., Lipkind, G. M., Fozzard, H. A., and Dudley, S., Jr. (1998) Predominant interactions between μ-conotoxin Arg-13 and the skeletal muscle Na^+ channel localized by mutant cycle analysis, *Biochemistry 37*, 4407−4419.
23. Hamill, O. P., Marty, A., Neher, E., Sakmann, B., and Sigworth, F. J. (1981) Improved patch-clamp techniques for high-resolution current recording from cells and cell-free membrane patches, *Pfluegers Arch. 391*, 85−100.
24. Stephan, M. M., Potts, J. F., and Angew, W. S. (1994) The μ1 skeletal muscle sodium channel: mutation E403Q eliminated sensitivity to tetrodotoxin but not to μ-conotoxin GIIIA and GIIIB, *J. Membr. Biol. 137*, 1−8.
25. French, R. J., and Dudley, S. C., Jr. (1999) Pore-blocking toxins as probes of voltage-dependent channels, *Methods Enzymol. 294*, 575−605.
26. Chahine, M., Sirois, J., Marcotte, P., Chen, L.-Q., and Kallen, R. G. (1998) Extrapore residues of the S5−S6 loop of domain 2 of the voltage-gated skeletal muscle sodium channel (rSkM1) contribute to the μ-conotoxin GIIIA binding site, *Biophys. J. 75*, 236−246.
27. Dudley, S. C., Chang, N., Hall, J., Lipkind, G., Fozzard, H. A., and French, R. J. (2000) μ-Conotoxin GIIIA interactions with he voltage-gated Na^+ Channel predict a clockwise arrangement of the domains, *J. Gen. Physiol. 116*, 679−690.
28. Li, R. A., Ennis, I. L., Dudley, S. C., French, R. J., Tomaselli, G. F., and Marbán, E. (2001) Clockwise domain arrangement of the sodium channel revealed by the docking orientation of μ-conotoxin, *J. Biol. Chem. 276*, 11072−11077.
29. Li, R. A., Ennis, I. L., Tomaselli, G. F., French, R. J., and Marbán, E. (1900) Characterization of the molecular interactions between μ-conotoxin (μ-CTX) and domain II P−S6 residues of the rat skeletal muscle (rSkM1) Na^+ channels, *Circulation 102*, II-264.

BI010077F